

Effect of defect size on P-S-N curves in Very-High-Cycle Fatigue

*Original*

Effect of defect size on P-S-N curves in Very-High-Cycle Fatigue / Paolino, Davide S.; Tridello, Andrea; Chiandussi, Giorgio; Rossetto, Massimo. - In: PROCDIA STRUCTURAL INTEGRITY. - ISSN 2452-3216. - ELETTRONICO. - 7:(2017), pp. 335-342. [10.1016/j.prostr.2017.11.097]

*Availability:*

This version is available at: 11583/2694754 since: 2019-04-30T16:58:19Z

*Publisher:*

Elsevier

*Published*

DOI:10.1016/j.prostr.2017.11.097

*Terms of use:*

This article is made available under terms and conditions as specified in the corresponding bibliographic description in the repository

*Publisher copyright*

(Article begins on next page)

3rd International Symposium on Fatigue Design and Material Defects, FDMD 2017, 19-22  
September 2017, Lecco, Italy

## Effect of defect size on P-S-N curves in Very-High-Cycle Fatigue

Davide S. Paolino<sup>a\*</sup>, Andrea Tridello<sup>a</sup>, Giorgio Chiandussi<sup>a</sup>, Massimo Rossetto<sup>a</sup>

<sup>a</sup>*Politecnico di Torino, Department of Mechanical and Aerospace Engineering, Corso Duca degli Abruzzi 24, Turin 10129, Italy*

---

### Abstract

It is well-known that internal defects play a key role in the Very-High-Cycle Fatigue (VHCF) response of metallic materials. VHCF failures generally nucleate from internal defects, whose size strongly affects the material strength and life. Therefore, S-N curves in the VHCF regime are defect size dependent and the scatter of fatigue data is significantly influenced by the statistical distribution of the defect size within the material.

The present paper proposes an innovative approach for the statistical modeling of Probabilistic-S-N (P-S-N) curves in the VHCF regime. The proposed model considers conditional P-S-N curves that depend on a specific value of the initial defect size. From the statistical distribution of the initial defect size, marginal P-S-N curves are estimated and the effect of the risk-volume on the VHCF response is also modeled. Finally, the paper reports a numerical example that quantitatively illustrates the concepts of conditional and marginal P-S-N curves and that shows the effect of the risk-volume on the VHCF response.

Copyright © 2017 The Authors. Published by Elsevier B.V.

Peer-review under responsibility of the Scientific Committee of the 3rd International Symposium on Fatigue Design and Material Defects.

**Keywords:** Random fatigue limit; Crack growth; Paris' law

---

---

\* Corresponding author. Tel.: +39-011-090-5746; fax: +39-011-090-6999.

E-mail address: [davide.paolino@polito.it](mailto:davide.paolino@polito.it)

## 1. Introduction

In many industrial fields (aerospace, railway, energy, automotive, marine), machinery components experience Very-High-Cycle Fatigue (VHCF) in-service conditions. A reliable design against VHCF failure is of utmost importance in these cases. In the last decades, a great effort has been made in order to collect VHCF data and to provide designers with reliable information on the VHCF response of different metallic materials. A number of models have been proposed in the literature (see, e.g., the review by Li, 2012), in order to quantify either the VHCF strength or the material fatigue limit. However, randomness of VHCF data has been rarely taken into account and the available statistical models have been prevalently devoted to the description of the random transition between High-Cycle Fatigue (HCF) and VHCF (Sakai et al, 2010; Harlow, 2011). A general probabilistic model, which can model both the transition HCF-VHCF and the possible presence of a fatigue limit, has been first proposed in Paolino et al. (2013) and Paolino et al. (2016). The model has been recently exploited in Paolino et al. (2016) for the statistical description of the VHCF response, on the basis of the hydrogen embrittlement theory proposed by Murakami (Murakami, 2002).

The present paper extends the approach in Paolino et al. (2016) to the different weakening mechanisms that have been proposed in the literature for explaining the formation of the so-called Fine Granular Area (FGA) around the initial defect. The FGA (also called Optically Dark Area or ODA by Murakami, Granular Bright Facet or GBF by Shiozawa and Rough Surface Area or RSA by Ochi) plays a major role in the VHCF response, since its formation consumes more than the 95% of the VHCF life. Researchers dispute about the actual mechanism behind the FGA formation (see, e.g., Li, 2016), but they unanimously accept that, within the FGA, crack can grow even if the Stress Intensity Factor (SIF) is below the SIF threshold for crack growth.

In the present paper, the reduction of the SIF threshold within the FGA is mechanistically modeled according to Paolino et al. (2017) and in agreement with the different weakening mechanisms proposed in the literature. Furthermore, since fatigue is scattered by nature, randomness of VHCF data is also taken into account and statistically modeled through originally defined Probabilistic-S-N (P-S-N) curves. The proposed model considers conditional P-S-N curves that depend on a specific value of the initial defect size. From the statistical distribution of the initial defect size, marginal P-S-N curves are estimated and the effect of the risk-volume on the VHCF response is also modeled. Finally, the paper reports a numerical example that quantitatively illustrates the concepts of conditional and marginal P-S-N curves and that shows the effect of the risk-volume on the VHCF response.

### Nomenclature

FGA	Fine Granular Area
SIF	Stress Intensity Factor
LEV	Largest Extreme Value distribution
HV	Vickers Hardness
$a_c, a_d, a_0, a_{FGA}, a_{FiE}$	projected areas of defects
$c_{th,g}, \alpha_{th,g}, c_{th,r}, \alpha_{th,r}$	parameters involved in SIF thresholds
$c_Y, m_Y, n_Y, \mu_{\sqrt{A}}, \sigma_{\sqrt{A}}, \sigma_{K_{th,g}}, \sigma_Y$	parameters of statistical distributions
$c_I, m_I, c_{II}, m_{II}, c_{III}, m_{III}, c_S, m_S$	Paris' constants in the three stages of crack growth
$F_{\sqrt{A_0,V}}, f_{\sqrt{A_0,V}}, F_{S_I \sqrt{a_{d,0}}}$	statistical distributions
$k_d, k_{th,g}, k_{th,l}, k_{th,r}$	relevant SIF values
$n_f, N_f$	number of cycles to failure
$n_I, n_{II}, n_{III}$	number of cycles in the three stages of crack growth
$s$	applied stress amplitude
$V, V_{exp}$	risk-volumes

## 2. Methods

In Section 2.1, a general expression for modeling the crack growth rate from the initial defect up to the VHCF failure is presented. In Section 2.2, the statistical distribution of the defect size and the related size-effects are analyzed and discussed. Finally, in Section 2.3, the statistical distribution of the fatigue limit is analytically defined and a model for the fatigue limit as a function of the risk-volume is proposed.

In the following, according to Paolino et al. (2017),  $k_{th,g}$  denotes the global SIF threshold,  $k_{th,r}$  denotes the reduction SIF,  $k_d$  denotes the SIF for an internal defect,  $k_{th,l}$  denotes the local SIF threshold (i.e.,  $k_{th,l} = k_{th,g} - k_{th,r}$ ),  $a_0$  is the projected area of the initial defect and  $a_{FGA}$  is the projected area of the FGA.

### 2.1. Crack growth rate within the FGA

In the VHCF literature (Tanaka and Akiniwa, 2002; Marines-Garcia et al., 2008; Su et al., 2017), the crack growth rate within the FGA is commonly modeled with the Paris' law. Three stages can be present in the crack growth rate diagram related to a VHCF failure from internal defect (Fig. 1):

- Stage I: the below-threshold region within the FGA, from  $k_{a_0}$  (SIF associated to the initial defect) up to  $k_{th,g}$ ;
- Stage II: the steady stage, from the border of the FGA (SIF equal to  $k_{th,g}$ ) up to the border of the fish-eye (with SIF equal to  $k_{FiE}$ );
- Stage III: the unsteady stage, beyond the fish-eye border (with SIF larger than  $k_{FiE}$ , up to the failure).

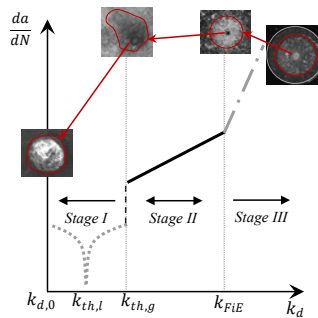


Fig. 1. The three stages of crack propagation in a crack growth rate diagram for VHCF failures from internal defects.

For a stress ratio equal to -1, the modified Paris' law proposed by Donahue et al. (1972) is considered to model the crack growth within the FGA:

$$\frac{da}{dN} = c_I (k_d - k_{th,l})^{m_I}, \quad (1)$$

where  $c_I$  and  $m_I$  are the Paris' constants related to Stage I, from the initial defect size  $\sqrt{a_0}$  up to  $\sqrt{a_{FGA}}$ .

According to (Tanaka and Akiniwa, 2002; Marines-Garcia et al., 2008; Su et al., 2017), in Stage II, from the border of the FGA up to the border of the fish-eye (with size  $\sqrt{a_{FiE}}$ ), the crack growth rate follows the conventional Paris' law:

$$\frac{da}{dN} = c_{II} k_d^{m_{II}}, \quad (2)$$

where  $c_{II}$  and  $m_{II}$  are the two Paris' constants related to Stage II, from  $\sqrt{a_{FGA}}$  up to  $\sqrt{a_{FiE}}$ .

Generally, crack propagates beyond the fish-eye border until it reaches the border of the final fracture, with size  $\sqrt{a_c}$ . In these cases, a third stage of crack propagation is visible on the fracture surfaces and it can be modeled again with the conventional Paris' law (Su et al., 2017):

$$\frac{da}{dN} = c_{III} k_d^{m_{III}}, \quad (3)$$

where  $c_{III}$  and  $m_{III}$  are the two Paris' constants related to Stage III, from  $\sqrt{a_{FiE}}$  up to  $\sqrt{a_c}$ . It is worth to note that, if the final fracture occurs when the crack size reaches the border of the fish-eye, Stage III can be neglected.

The number of cycles to failure,  $N_f$ , can be expressed as the sum of the number of cycles consumed within the three stages of propagation:

$$n_f = n_I + n_{II} + n_{III}. \quad (4)$$

Following the VHCF literature (see, e.g., Su et al., 2017),  $n_I$  can be estimated by subtracting, from the experimental  $n_f$ , the numbers of cycles consumed in Stages II and III, which are obtained through integration of Eqs. (2) and (3), respectively.

According to Paolino et al. (2017), the experimental  $n_I$  values ( $n_{I,exp}$ ) can be used for the estimation of the Paris' constants  $c_I$ ,  $m_I$  and of the parameters  $c_{th,r}$  and  $\alpha_{th,r}$  involved in the expression of the  $k_{th,l}$ . Parameter estimates are obtained through the nonlinear Least Squares Method by minimizing the sum of squared percent errors between the experimental  $\log_{10}(n_{I,exp})$  values and the estimated  $\log_{10}(n_{I,est})$  values computed through integration of Eq. (1). Finally, an estimate of the fatigue limit can be defined, according to the procedure described in Paolino et al. (2017).

## 2.2. Statistical distribution of the initial defect size and related size-effect

Size-effects significantly affect the VHCF response of materials (Furuya, 2011; Tridello et al., 2015): the larger the risk-volume (volume of material subjected to a stress larger than the 90% of the maximum stress), the larger the probability of large defects, with a subsequent reduction of the VHCF strength. The dependency between the fatigue limit and the risk-volume is generally modeled by taking into account the statistical distribution of the internal defect size. According to the VHCF literature (Murakami, 2002), the defect originating failure can be considered as the largest defect present within the specimen risk-volume and, therefore, in a statistical framework the internal defect size random variable (rv) follows a Largest Extreme Value (LEV) distribution.

The cumulative distribution function (cdf) of the LEV distribution is reported in Eq. (5): it provides the probability of an internal defect with size smaller than  $\sqrt{a_0}$  in a volume  $V$  larger than the risk-volume of the tested specimens ( $V_{exp}$ ).

$$F_{\sqrt{a_0}|V}(\sqrt{a_0}; V) = \left( \exp \left( - \exp \left( - \frac{\sqrt{a_0} - \mu_{\sqrt{A}}}{\sigma_{\sqrt{A}}} \right) \right) \right)^{\frac{V}{V_{exp}}}, \quad (5)$$

where  $\mu_{\sqrt{A}}$  and  $\sigma_{\sqrt{A}}$  are the two constant parameters of the distribution. The probability density function (pdf) of the LEV distribution,  $f_{\sqrt{a_0}|V}$ , is expressed by:

$$f_{\sqrt{a_0}|V}(\sqrt{a_0}; V) = \frac{1}{\sigma_{\sqrt{A}}} \exp \left( - \frac{\sqrt{a_0} - (\mu_{\sqrt{A}} + \log(V/V_{exp}))}{\sigma_{\sqrt{A}}} \right) - \exp \left( - \frac{\sqrt{a_0} - (\mu_{\sqrt{A}} + \log(V/V_{exp}))}{\sigma_{\sqrt{A}}} \right). \quad (6)$$

According to Murakami (2002), the parameters of the LEV distribution can be estimated from the defect sizes  $\sqrt{a_0}$  measured on the fracture surfaces of the tested specimens (i.e., with  $V = V_{exp}$  in Eqs. (5) and (6)).

### 2.3. Statistical distribution of the fatigue limit and related size-effect

According to Paolino et al. (2016) the cdf of the fatigue limit for a given defect size (conditional VHCF limit) can be expressed as:

$$F_{S_l|\sqrt{a_0}}(s_l; \sqrt{a_0}) = \Phi\left(\frac{1}{\sigma_{K_{th,g}}}\left(\log_{10}(s_l) - \log_{10}\left(c_{th,g} \frac{c_{s_l}(HV+120)}{\sqrt{a_0}^{1/2-\alpha_{th,g}}}\right)\right)\right) = \Phi\left(\frac{\log_{10}(s_l) - \mu_l(\sqrt{a_0})}{\sigma_l}\right), \quad (7)$$

where  $\Phi(\cdot)$  denotes the standardized Normal cdf,  $c_{th,g}$ ,  $\alpha_{th,g}$  and  $\sigma_{K_{th,g}}$  are the parameters involved in the statistical distribution of the global SIF threshold (Paolino et al., 2016; Paolino et al., 2017),  $HV$  is the Vickers hardness of the

material and  $c_{s_l} = \left(\frac{(1/2-\alpha_{th,g})0.5\sqrt{\pi}}{(\alpha_{th,g}-\alpha_{th,r})c_{th,r}}\right)^{\frac{1/2-\alpha_{th,g}}{1/2-\alpha_{th,r}}} \frac{\alpha_{th,g}-\alpha_{th,r}}{0.5\sqrt{\pi}(1/2-\alpha_{th,r})}$ .

The cdf of the fatigue limit as a function of the risk-volume (marginal VHCF limit) can be obtained from the definition of marginal cdf and by taking into account the defect size distribution in Eq. (6):

$$F_{S_l|V}(s_l; V) = \int_0^\infty F_{S_l|\sqrt{a_0}}(s_l; \sqrt{a_0}) f_{\sqrt{a_0}|V}(\sqrt{a_0}; V) d\sqrt{a_0}. \quad (8)$$

### 2.4. P-S-N curves and related size-effect

The P-S-N curves statistically model the VHCF material response in the fatigue limit region and in the finite fatigue life region.

Eqs. (7) and (8) model the randomness in the fatigue limit region. According to (Paolino et al., 2016), the cdf of the finite fatigue life for given initial defect and applied stress  $s$  (conditional finite VHCF life),  $N_{f,<\infty}|(s, \sqrt{a_0})$ , can be expressed as:

$$F_{N_{f,<\infty}|(s,\sqrt{a_0})}(n_f; s, \sqrt{a_0}) = \Phi\left(\frac{\log_{10}(n_f) - (c_Y + m_Y \log_{10}(s) + n_Y \log_{10}(\sqrt{a_0}))}{\sigma_Y}\right) = \Phi\left(\frac{\log_{10}(n_f) - \mu_Y(s, \sqrt{a_0})}{\sigma_Y}\right), \quad (7)$$

where  $\sigma_Y$  denotes a constant standard deviation and  $c_Y$ ,  $m_Y$  and  $n_Y$  are three constant parameters that can be estimated from the experimental failures through the Least Squares Method.

According to the probabilistic model “One failure mode due to one cause with fatigue limit” described in (Paolino et al., 2013), the cdf of the fatigue life (finite as well as infinite) for given initial defect and applied stress  $s$  (conditional VHCF life),  $N_f|(s, \sqrt{a_0})$ , is given by:

$$F_{N_f|(s,\sqrt{a_0})}(n_f; s, \sqrt{a_0}) = F_{S_l|\sqrt{a_0}}(s; \sqrt{a_0}) F_{N_{f,<\infty}|(s,\sqrt{a_0})}(n_f; s, \sqrt{a_0}). \quad (8)$$

The  $\alpha$ -th quantile of the conditional VHCF life,  $n_{f,(s,\sqrt{a_0}),\alpha}$ , can be obtained by substituting  $F_{N_f|(s,\sqrt{a_0})}(n_f; s, \sqrt{a_0})$  with  $\alpha$  and by solving the equation with respect to  $n_f$  for different values of  $s$ :

$$n_{f,(s,\sqrt{a_0}),\alpha} = 10^{\mu_Y(s,\sqrt{a_0}) + \sigma_Y \Phi^{-1}\left(\alpha / \Phi\left(\frac{\log_{10}(s) - \mu_l(\sqrt{a_0})}{\sigma_l}\right)\right)}, \quad (9)$$

where  $s$  must be larger than  $10^{\mu_l(\sqrt{a_0}) + \sigma_l \Phi^{-1}(\alpha)}$  in order to have finite values of  $n_{f,(s,\sqrt{a_0}),\alpha}$ . Eq. (9) thus provides the P-S-N curves given the initial defect size (conditional P-S-N curves).

The cdf of the VHCF life as a function of the risk-volume (marginal VHCF life) can be obtained from the definition of marginal cdf and by taking into account the defect size distribution in Eq. (6):

$$F_{N_f|(s,V)}(n_f; s, V) = \int_0^\infty F_{N_f|(s,\sqrt{a_0})}(n_f; s, \sqrt{a_0}) f_{\sqrt{a_0}|V}(\sqrt{a_0}; V) d\sqrt{a_0}. \quad (10)$$

The  $\alpha$ -th quantile of the fatigue life can be obtained by substituting  $F_{N_f|(s,V)}(n_f; s, V)$  with  $\alpha$  and by solving the equation with respect to  $s$  for different values of  $n_f$ . Eq. (10) thus provides the P-S-N curves of the material for a given risk-volume (marginal P-S-N curves).

### 3. Application to an experimental dataset

The models proposed in Section 2 are here applied to an experimental dataset. VHCF tests are carried out on Gaussian specimens (Tridello et al., 2015) made of an AISI H13 steel with Vickers hardness  $560 \text{ kgf/mm}^2$  and  $V_{exp} = 2300 \text{ mm}^3$ . Details on the testing setup and on the tested material are reported in Tridello et al. (2015) and in Tridello et al. (2016) and they will not be recalled here for the sake of brevity. Twelve specimens are loaded at constant stress amplitude up to failure. The number of cycles to failure ranges from  $4.2 \cdot 10^7$  to  $3.85 \cdot 10^9$  cycles. The initial defect sizes ( $\sqrt{a_0}$ ) and the FGA sizes ( $\sqrt{a_{FGA}}$ ) are measured from pictures taken by a Scanning Electron Microscope (SEM) and by an optical microscope. In order to take into account the stress variation within the  $V_{exp}$ , the local stress amplitude in the vicinity of the initial defect is considered as the stress amplitude applied during the test. The local stress amplitudes are in the range 500 - 635 MPa.

The parameters  $c_{th,g}$ ,  $\alpha_{th,g}$ ,  $\sigma_{K_{th,g}}$  and  $c_{s_l}$ , which are involved in the fatigue limit expressions (Eqs. (7) and (8)), are estimated according to the procedure described in Paolino et al. (2017). Fig. 2a shows the  $k_{th,g}$  values with respect to  $\sqrt{a_{FGA}}$  together with the estimated model ( $k_{th,g,\alpha}$  is the  $\alpha$ -quantile of the Global SIF threshold,  $HV$  is the material Vickers Hardness and  $\Phi^{-1}$  is the inverse cumulative distribution function of a standardized Normal distribution). Fig. 2b shows the conditional VHCF limit curves as a function of the initial defect size ( $s_{l,\sqrt{a_0},\alpha}$  is the  $\alpha$ -quantile of the conditional fatigue limit). The 0.1-th and the 0.9-th quantiles are also depicted in Fig. 2.

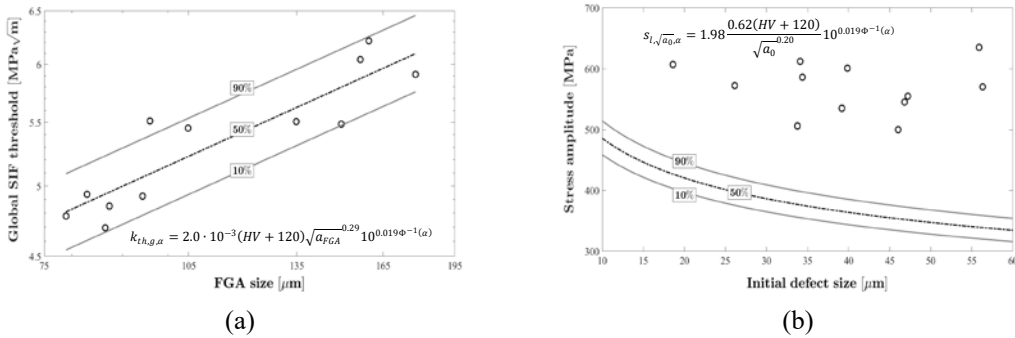


Fig. 2. (a) Global SIF threshold vs. FGA size. (b) Conditional VHCF limit vs. initial defect size.

According to Fig. 2b, the fatigue limit decreases with the initial defect size (Murakami, 2002; Furuya, 2011). The estimated fatigue limit curves are below the experimental failures, as expected from the definition of fatigue limit. The proposed model is therefore effective in the estimation of the fatigue limit variation with respect to the initial defect size and ensures a reliable safety margin with respect to the experimental failures.

The distribution of initial defect size is estimated according to Murakami (2002). Fig. 3a shows the Gumbel plot of the measured  $\sqrt{a_0}$  values together with the estimated LEV cdf. Parameter estimation is carried out by considering  $V = V_{exp} = 2300 \text{ mm}^3$ . From the initial defect size distribution and according to Eq. (8), the 0.1-th, 0.5-th and the 0.9-th quantiles of the fatigue limit are estimated for risk-volumes larger than  $V_{exp}$  and then depicted in Fig. 3b.

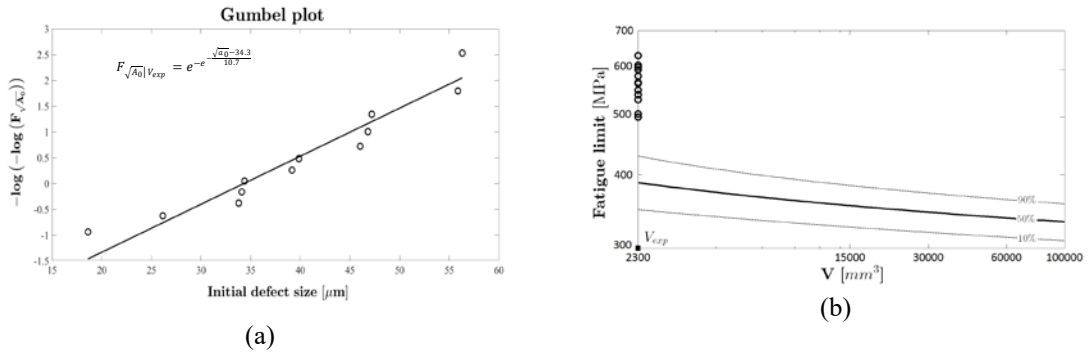


Fig. 3. (a) Gumbel plot of the initial defect size. (b) Variation of the marginal VHCF limit with the risk-volume.

Fig. 4 shows a plot of the conditional P-S-N curves. Fig. 4a plots the 0.1-th, the 0.5-th and the 0.9-th curves corresponding to an initial defect with median size; whereas Fig. 4b depicts the median curves for values of the initial defect size ranging from 15  $\mu\text{m}$  to 60  $\mu\text{m}$ .

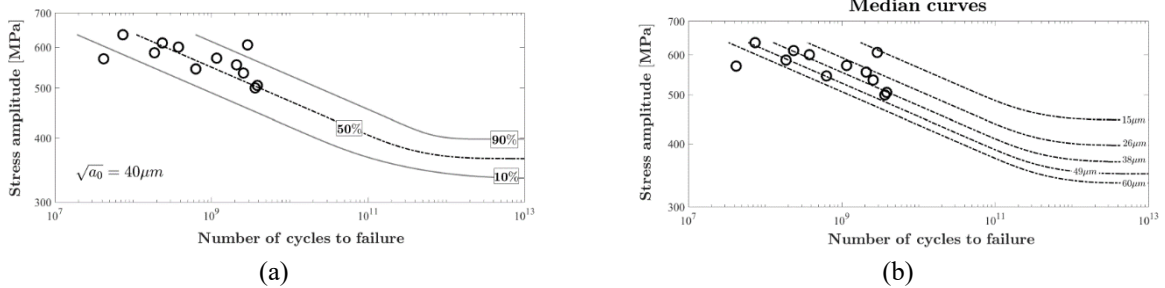


Fig. 4. Conditional P-S-N curves: (a) 80% confidence band for a median defect size; (b) median curves for different defect sizes.

Finally, by taking into account the defect size distribution, the marginal P-S-N curves (no more conditioned to the inclusion size, as in Fig. 4) are estimated. Fig. 5a plots the 0.1-th, the 0.5-th and the 0.9-th curves corresponding to a risk-volume equal to  $V_{exp} = 2300 \text{ mm}^3$ ; whereas Fig. 5b depicts the median curves the risk-volume larger than  $V_{exp}$ .

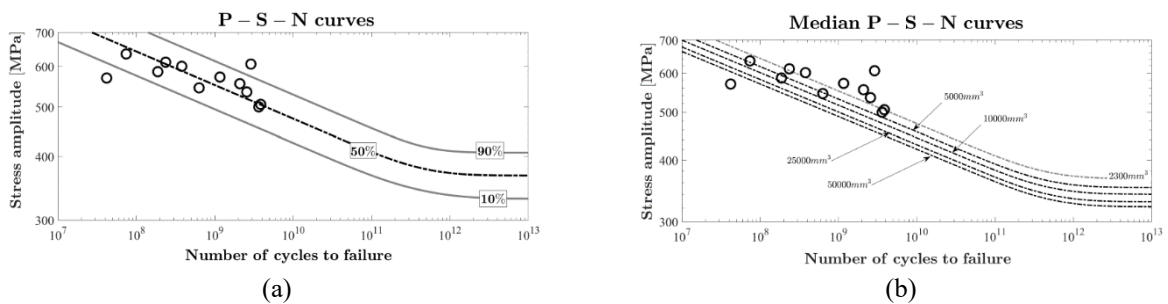


Fig. 5. Marginal P-S-N curves: (a) 80% confidence band for a risk-volume equal to  $V_{exp}$ ; (b) median curves for larger risk-volumes.

Marginal P-S-N curves reported in Fig. 5 can be used for component design, since they are not conditioned to a specific value of inclusion size (Fig. 4). In particular, the model in Fig. 5b can be used to predict the VHCF life of components characterized by risk-volumes (up to 100000  $\text{mm}^3$ ) significantly larger than risk-volumes of specimens commonly tested.



#### 4. Conclusions

In the present paper, a general model for the P-S-N curves in the VHCF regime was proposed. The statistical distribution of the P-S-N curves for a given initial defect size (conditional P-S-N curves) and the P-S-N curves as a function of the risk-volume (marginal P-S-N curves) were defined. The proposed model permitted to take into account defect size-effects on the VHCF response and to predict the P-S-N curves of components characterized by large risk-volumes.

The model was successfully applied to an experimental dataset. The P-S-N curves as a function of the defect size and as a function of the risk-volume were estimated and were in agreement with the experimental data: for the tested risk-volume, about 80% of data were within the estimated 80% confidence band.

The proposed model could be effectively adopted for the estimation of the P-S-N curves when designing large components subjected to VHCF.

#### References

- Donahue, R. J., Clark, H. M., Atanmo, P., Kumble, R., McEvily, A. J., 1972. Crack opening displacement and the rate of fatigue crack growth. *International Journal of Fracture Mechanics* 8, 209-219.
- Furuya, Y., 2011. Notable size effects on very high cycle fatigue properties of high-strength steel. *Materials Science and Engineering: A* 528, 5234-5240.
- Harlow, D. G., 2011. Statistical characterization of bimodal behaviour. *Acta Materialia* 59, 5048-5053.
- Li, S. X., 2012. Effects of inclusions on very high cycle fatigue properties of high strength steels. *International Materials Reviews* 57, 92-114.
- Li, Y. D., Zhang, L. L., Fei, Y. H., Liu, X. Y., Li, M. X., 2016. On the formation mechanisms of fine granular area (FGA) on the fracture surface for high strength steels in the VHCF regime. *International Journal of Fatigue* 82, 402-410.
- Marines-Garcia, I., Paris, P. C., Tada, H., Bathias, C., Lados, D., 2008. Fatigue crack growth from small to large cracks on very high cycle fatigue with fish-eye failures. *Engineering Fracture Mechanics* 75, 1657-1665.
- Murakami, Y., 2002. *Metal fatigue: effects of small defects and nonmetallic inclusions*. Elsevier, Oxford, UK.
- Paolino, D. S., Chiandussi G., Rossetto, M., 2013. A unified statistical model for S-N fatigue curves: probabilistic definition. *Fatigue and Fracture of Engineering Materials and Structures* 36, 187-201.
- Paolino, D. S., Chiandussi G., Rossetto, M., 2016. Statistical estimation of duplex S-N curves. *Key Engineering Materials* 664, 285-294.
- Paolino, D. S., Tridello, A., Chiandussi, G., Rossetto, M., 2016. S-N curves in the very-high-cycle fatigue regime: statistical modeling based on the hydrogen embrittlement consideration. *Fatigue & Fracture of Engineering Materials & Structures* 39, 1319-1336.
- Paolino, D. S., Tridello, A., Chiandussi, G., Rossetto, M., 2017. A general model for crack growth from initial defect in Very-High-Cycle Fatigue. *Procedia Structural Engineering* 3, 411-423.
- Sakai, T., Sato, Y., Oguma, N., 2002. Characteristic S-N properties of high-carbon-chromium-bearing steel under axial loading in long-life fatigue. *Fatigue & Fracture of Engineering Materials & Structures* 25, 765-773.
- Sakai, T., Lian, B., Takeda, M., Shiozawa, K., Oguma, N., Ochi, Y., Nakajima, M., Nakamura, T., 2010. Statistical duplex S-N characteristics of high carbon chromium bearing steel in rotating bending in very high cycle regime. *International Journal of Fatigue* 32, 497-504.
- Su, H., Liu, X., Sun, C., Hong, Y., 2017. Nanograin layer formation at crack initiation region for very-high-cycle fatigue of a Ti-6Al-4V alloy. *Fatigue & Fracture of Engineering Materials & Structures* 40, 979-993.
- Tanaka, K., Akiniwa, Y., 2002. Fatigue crack propagation behaviour derived from S-N data in very high cycle regime. *Fatigue & Fracture of Engineering Materials & Structures* 25 775-784.
- Tridello, A., Paolino, D. S., Chiandussi, G., Rossetto, M., 2015. VHCF response of AISI H13 steel: assessment of size effects through Gaussian specimens. *Procedia Engineering* 109, 121-127.
- Tridello, A., Paolino, D. S., Chiandussi, G., Rossetto, M., 2016. Different inclusion contents in H13 steel: Effects on VHCF response of Gaussian specimens. *Key Engineering Materials* 665, 49-52.